Parameter Optimization via CMA-ES for Implementation in the Active Control of Magnetic Pillar Arrays

Gaysornkaew, Suparat
Dept. of Mechanical and Aerospace Engineering, Kyushu University

Vargas, Danilo Vasconcellos
Dept. of Informatics, Kyushu University

Tsumori, Fujio
Dept. of Aeronautics and Astronautics, Kyushu University

https://hdl.handle.net/2324/4752556

KYUSHU UNIVERSITY

Parameter Optimization via CMA-ES for Implementation in the Active Control of Magnetic Pillar Arrays

Suparat Gaysornkaew
Dept. of Mechanical and Aerospace Engineering
Kyushu University
Fukuoka, Japan
gaysornkaew.suparat.818@s.kyushu-u.ac.jp

Danilo Vasconcellos Vargas
Dept. of Informatics
Kyushu University
Fukuoka, Japan
vargas@inf.kyushu-u.ac.jp

Fujio Tsumori
Dept. of Aeronautics and Astronautics
Kyushu University
Fukuoka, Japan
tsumori@aero.kyushu-u.ac.jp

Abstract—Pillared surfaces are the products of a surface modification technique that allow the implementation of active control methods by an outer source such as magnetic fields. Pillar arrays with magnetic tips exhibit different characteristics depending on the initial positional arrangement of the pillars and/or the environmental magnetic field conditions. This study develops methods for simulation and parameter optimization by machine learning to aid the investigation of pillar behaviors in various combinations of initial positions and magnetic fields. Optimization is performed using the co-variance adaptation evolution strategy (CMA-ES). The algorithm is tested to obtain preliminary results: (1) the maximum size of the pillar pitch at a given magnetic field; (2) the initial pillar arrangement of a 3-pillar unit cell and three settings of applied magnetic field–each corresponds to a predefined contact state of a three-stage paring pattern.

Index Terms—magnetic pillar arrays, simulation, machine learning, CMA-ES

I. INTRODUCTION

Surface engineering is currently of high importance for not only scientific or industrial research but also daily appliances. Some well-known surface engineering technologies include wear-resistant surfaces, hydrophilic or hydrophobic surfaces, adhesive surfaces, and antifouling surfaces. These functional surfaces can be engineered by modifying surface properties of materials chemically or physically.

For physical surface modification, implementation of mechanical structure such as pillar arrays is one of the techniques that provide advantages in various fields of applications–from cell analysis [1]–[2] to self-cleaning surfaces [3]. In biomimetics, pillar arrays are often used to model some real micro- or nano-scale biological surfaces in the studies of functional surfaces like artificial cilia [4]–[5], Lotus-leaf- [6]–[7] or gecko-foot-mimetic surfaces [8]–[9].

The functionality of pillared surfaces can be further improved by equipping them with some control methods. For miniaturized structure, control methods by an outer source is often used as it is difficult or even impractical in some cases to attach control equipment to the body of the structure.
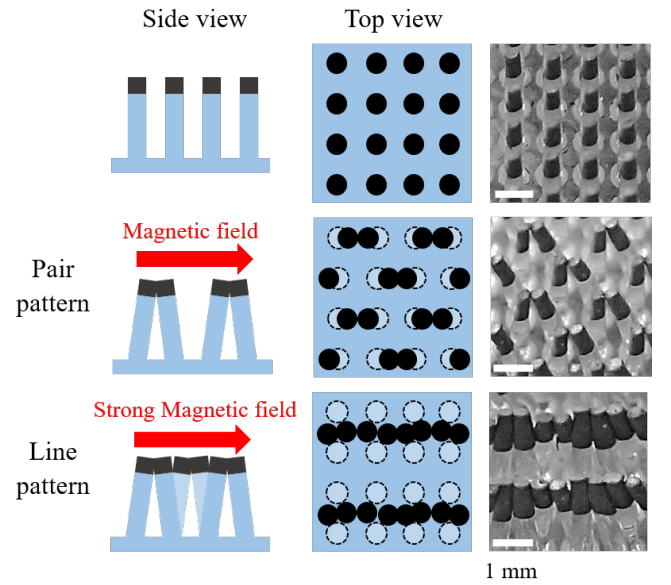
Fig. 1. Pillar arrays with magnetic tips in static magnetic field.

Magnetic elastomer, an elastic structure with magnetic powder embedded inside, is one of those methods that allows the actuation control by magnetic fields. Some examples include magnetic cilia [10]–[13] and magnetic crawler [14].

In previous work [15], the active control method by magnetic fields using magnetic particles embedded in the tips of elastic pillar arrays was studied. It was found that the response of pillar arrays could be managed by controlling the applied magnetic fields. The results showed pillar patterns, namely pair pattern and line pattern, under different magnetic field strengths as illustrated in Fig. 1. The deformation patterns of a 45×45 pillar array surface could be utilized for a dynamic object manipulation as shown in Fig. 2.

The results also suggested that the pillar behaviors are dependent on the initial parameters such as their sizes and positional arrangements in addition to the environment conditions
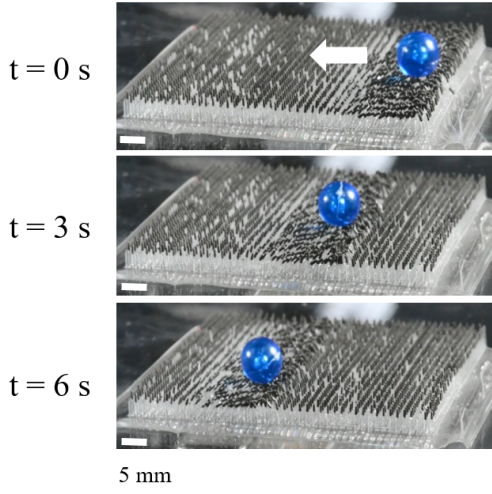
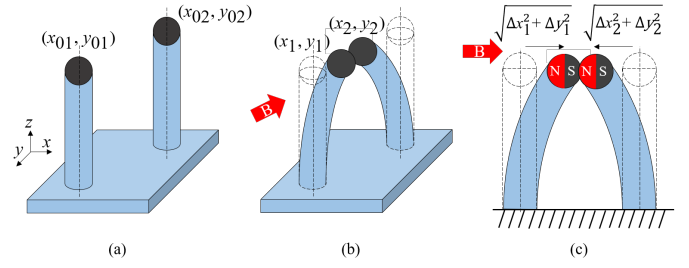Fig. 2. Object manipulation on a large magnetic pillared surface.

Fig. 3. Simulation model of magnetic pillar arrays. (a) Without magnetic field. (b) Under a magnetic field. (c) Deformation due to the magnetic force.

(i.e., magnetic field strengths and directions). This inspired the idea to use these influential parameters to design and control the behavior of a large magnetic pillared surface to achieve more functional dynamic movements.

The question rises as how to determine the values of the parameters. To answer it, more investigations should be conducted on how pillar arrays with different arrangements response to various magnetic field conditions. However, investigation by pure experiments would consume massive amount of time and cause large amount of material waste. It is much faster and more efficient to study the problem through simulations and machine learning optimization tools to filter out methods that could lead to failure.

Therefore, this present study aims to make use of the co-variance matrix adaptation evolution strategy (CMA-ES) [16], a parameter optimization method that promotes machine learning, in the development of the active control of magnetic pillar arrays. The method can also be useful for designing some other magnetically controllable 3D printed structures as well as their deformations (i.e, 4D printed structures) like ones from these studies [17]–[20].

In this work, we simulated the behaviors of a small sized elastic pillar array with magnetic tips and implemented a machine learning process via CMA-ES to investigate: (1) the maximum pillar pitch in which two pillar tips contact at a given magnetic field strength and (2) the combination of initial position of the pillar arrays and magnetic field conditions that allows the pillars to display objective multistage pattern.

II. SIMULATION OF MAGNETIC PILLAR ARRAYS

The position of magnetic pillar tips on the x-y coordinate plane under the given magnetic field is simulated. The procedure is divided into two main sections, the physical modeling of magnetic pillars and the theoretical formulation of the pillar behavior.

A. Physical Modeling of Magnetic Pillars

The mathematical model used for the simulation is based upon the previous work [21]–[22]. The system for simulation consists of a collection of individual pillars and the environmental magnetic fields. Each pillar is modelled as an elastic cylindrical cantilever beam with a spherical magnetic bead attaching on its tip as shown in Fig. 3a. Here, every pillar is assumed to be identical in both chemical and physical properties.

B. Theoretical Formulation of Magnetic Pillar Behavior

With the presence of magnetic field, the magnetic bead on each pillar is magnetized and therefore, is carrying some potential energy due to its own magnetic dipole as well as that of the other magnetic beads of the surrounding pillars. The total magnetic dipole potential energy ($U_{magnetic}$) of the system can be described as in (1)

$$U_{magnetic} = -\sum_{j=1}^{N} \frac{1}{2} \mathbf{m}_j \mathbf{B}_j'$$ (1)

where N is the total number of pillars in the system. $\mathbf{m}_j$ is the dipole moment of the j th bead which is calculated using (2) and (3).

$$\mathbf{m}_j = \frac{4\pi}{\mu_0} \frac{(\mu - 1)}{(\mu + 2)} a_j \mathbf{B}_j$$ (2)

$$\mathbf{B}_j = \mathbf{B}_j' + \frac{\mu_0}{4\pi} \sum_{\substack{k=1 \\ k \neq j}}^{N} \left(\frac{3(\mathbf{m}_k \cdot \mathbf{r}_{kj})}{|\mathbf{r}_{kj}|^5} \mathbf{r}_{kj} - \frac{\mathbf{m}_k}{|\mathbf{r}_{kj}|^3} \right)$$ (3)

$\mathbf{B}_j'$ is the applied magnetic field at the j th bead. $\mathbf{m}_k$ is the dipole moment of k th bead. r_{kj} is the position vector from the k th bead to j th bead. a_j, μ_0, and μ is the pillar radius, the vacuum permeability, and the permeability of the bead material, respectively [23].

The magnetic force acting on the pillars causes them to bend resulting in elastic potential energy ($U_{elastic}$) which is calculated as in (4). x_j and y_j is the x and y component of the current tip position whereas x_{0j} and y_{0j} is the x and y component of the initial tip position of the j th pillar,

respectively. k is the spring constant of an elastic cylindrical pillar (cantilever).

$$U_{elastic} = \sum_{j=1}^{N} \frac{1}{2} k \left((x_j - x_{0j})^2 + (y_j - y_{0j})^2 \right) \quad (4)$$

The schematic diagram of pillar deformation is shown in Figs. 3b and 3c where $\Delta x_1 = x_1 - x_{01}$, $\Delta y_1 = y_1 - y_{01}$, and similarly for Δx_2 and Δy_2.

When the field strength is strong enough, the pillars attach to each other resulting in the potential energy due to the contact stress ($U_{contact}$). In this study, it is calculated based on the Hertzian contact of two spheres [24] as described in (5) and (6). α_{kj} is the distance that the surfaces of the spherical heads of k th and j th pillars are pressed into each other. a is the pillar radius.

$$U_{contact_{kj}} = \begin{cases} \frac{2}{15} \frac{E}{(1-v^2)} \sqrt{2a \cdot \alpha_{kj}^{\frac{5}{2}}}, & \text{if } \alpha_{kj} > 0 \\ 0, & \text{otherwise} \end{cases} \quad (5)$$

$$U_{contact} = \sum_{k=1}^{N} \sum_{\substack{j=1 \\ j \neq k}}^{N} U_{contact_{kj}} \quad (6)$$

Therefore, the total potential energy (U) can be described below in (7).

$$U = U_{magnetic} + U_{elastic} + U_{contact} \quad (7)$$

According to the minimum total potential energy principle of the system, the pillar arrays will arrange themselves in a formation that results in the lowest total potential energy. Hence, the position of the pillar tips could be found by evaluating the position of pillar arrays corresponding to the lowest potential energy at a given magnetic field which could be done using some computational methods. We used the steepest descent method [25] or CMA-ES which we implemented them in C++ or Python, respectively, because of their convergence property which is suitable for solving numerical optimization problems in this work.

III. IMPLEMENTATION OF MACHINE LEARNING

Fig. 4 shows the schematic diagram of the optimization algorithm for one generation in the evolution. In each generation, some number of sets of parameters to be optimized (referred to as off springs) are generated. Each set of parameters is fed to the simulation program to obtain the characteristics of pillar arrays under a specific magnetic field. The simulation results are then compared with the desired result to determine the value of the objective function which shall be minimized. From each generation, some healthy results that give the lowest objective function values are selected to be the parents of the next generation. Again, some number of new off springs are generated and the process continues until the objective function value is small enough. The best offspring of the last generation is selected as the final optimization result.
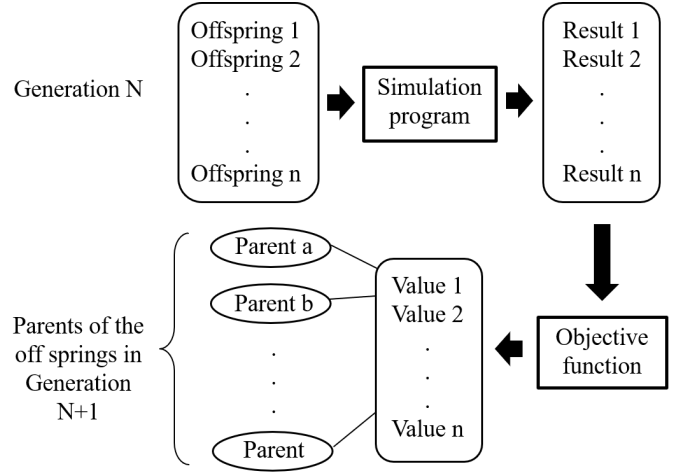

Fig. 4. Schematic diagram of the optimization algorithm for Generation N.

In this work, we could utilize CMA-ES from a Python library called 'cmaes' [26] to optimize the pitch between two pillars and to search for the combination of initial pillar positional arrangement and the environmental magnetic field that delivers the desired multistage pairing behavior. The library can be used on its own or through an automatic hyperparameter optimization framework Optuna [27].

A. Optimization of Pillar Pitch

A system of two pillars is evaluated. The pillars are constrained to only move along the x axis and the magnetic field is only applied in x-direction. The optimization parameters passed to the C++ simulation program are the x components of the initial position of each pillar. CMA-ES is used to find the pitch between two pillars that will result in their tips just touching each other (i.e., the maximum pitch) at the provided magnetic field strength. Here, the objective function returned the difference in mm of the simulated final distance between two pillars and the desired distance which is the pillar diameter in this case. Note that any two pillars of the same size contact if the distance between their tips becomes less than or equal to two times their radius, i.e., their diameter.

B. Parameter Search for Predefined Multistage Pairing

The optimization is executed on groups of parameters. Each group comprises of: (1) the change in initial position (Δx and Δy) of each pillar, and (2) sets of x and y components of magnetic field that when applied to the pillar arrays would result in the desired contact states. To evaluate n stages of pairing (contact), n sets of magnetic field conditions are needed–each one for each stage. Therefore, in a group, there are n sets of parameters, all with the same pillar positional arrangement but different magnetic field condition.

Each group of parameters is passed to the Python simulation program to obtain the pillar tip position corresponding to that particular group. The simulation result from each set (stage) in the group is compared with the previously specified contact state for that stage. The objective function combines
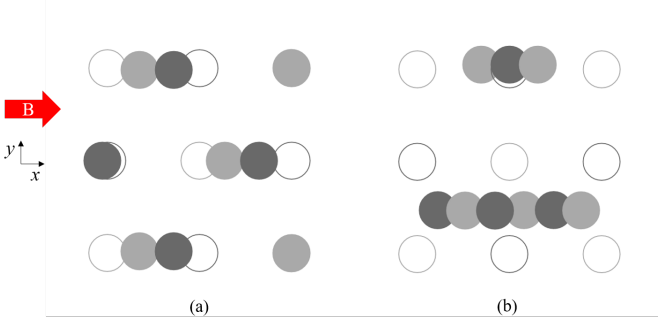
Fig. 5. Simulation results for the pillar arrays of the size 3×3 under a horizontal magnetic field. (a) Pair pattern at the field strength of 0.15 T. (b) Line pattern at the field strength of 0.30 T.
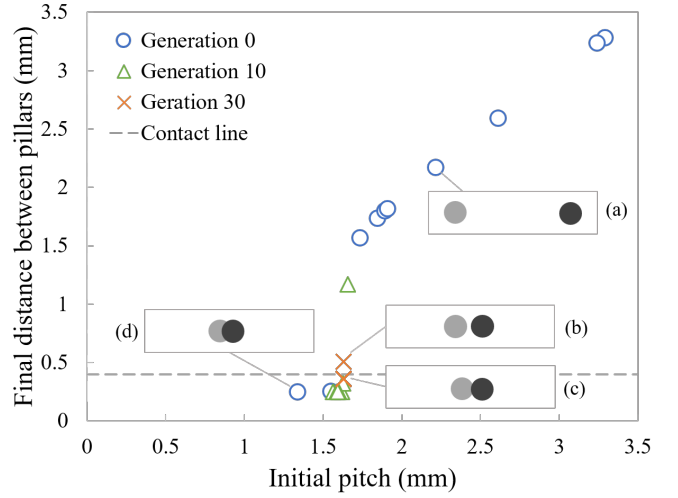

Fig. 6. Plot of random ten off springs from each Generation 0, 10, and 30 of the pillar pitch optimization at 0.3 T magnetic field and the final pillar state corresponding to the size of initial pitch: (a) Separated (b) Separated with a small gap (c) Pushed slightly into each other (d) Pushed into each other.

those comparison values from all sets and then, evaluates the similarity as a whole. The value returned from the objective function is minimized as the generation increased. After some generations, the group with the lowest objective function value is finally selected as the best combination.

IV. PRELIMINARY RESULTS

Preliminary results for the simulation and the implementation of machine learning are described in this section.

A. Simulation Results

The final position of the magnetic tips of 3×3 pillar arrays under a horizontal magnetic field (i.e, y-component of the magnetic field was zero) was simulated using C++ simulation program. Here, the pillars had the radius of 0.20 mm, the height of 3.0 mm, and the pitch of 1.0 mm. The results illustrated in Fig. 5 showed pair and line pattern at the magnetic field strength of 0.15 and 0.30 T, respectively. It was confirmed that the simulation output matched with the experimental results from the previous study in Fig. 1.

B. Optimization of Pillar Pitch

The size of the initial pillar pitch that resulted in two pillar tips just touching each other at a given magnetic field was investigated. The pillar size was 0.20 mm in radius and 3.0 mm in height. The optimization results after 30 generations suggested the best maximum pitch to be 0.941, 1.238, and 1.630 mm approximately for the magnetic field strength of 0.075, 0.15, and 0.30 T, respectively. The pitch increased as the field strength increased supporting the fact that a stronger magnetic force is capable of attracting two magnetic pillar heads from a further distance into contact.

Fig. 6 shows the pitch optimization results for the case of 0.30 T magnetic field. Ten random generated off springs from each 0th, 10th, and 30th generation were plotted having the size of their initial pitch as the x axis and their final distance between the two pillars as the y axis. The off springs of the 0th generation scattered over a large range. The range reduced rapidly in the later generations as the values of the off springs were approaching the solution. In 30th generation, the off springs grouped up around the value of the contact line which

was equal to 0.40 mm (two times pillar radius) where the pillar tips contacted.

The states of contact of the pillar tips depended on their initial pitch. The pillars did not contact if the pitch was too large (Figs. 6a and 6b). On the other hand, they were pushed into each other if the pitch was too small (Figs. 6c and 6d). The initial pitch that resulted in the final pillar tips contacted with the least area of the pillars being pushed into each other was considered as the best solution in the generation (Fig. 6d for Generation 0 and Fig. 6c for Generation 30).

C. Parameters Search for Three-stage Pairing

A system with a unit cell of three pillar arrays was evaluated. The pillar radius was 0.050 mm and the height was 0.50 mm. Here, three stages of the contact state of the pillars were specified as followed: (1) the tip of the first and the third pillar in the unit cell contacted to the tip of the third and the first pillar the neighboring cells, respectively, (2) the tips of the first and the second pillar contacted, and (3) the tips of the second and the third pillar contacted. The mechanism is portrayed in the column of desired mechanism in Fig. 7. The pillars in the unit cell are in color whereas the neighboring pillars are in white. The periodic change of this mechanism could create a dynamic movement that might be useful for conveying objects on the surface of the pillar tips.

The CMA-ES found the initial positional arrangement of the pillars in a unit cell when the applied magnetic field B was zero to be in a shallow V-like pattern as shown in yellow color in Fig. 7. The three magnetic field conditions that satisfied the previously specified three-stage pairing were: (1) 0.33 T horizontal (2) 0.80 T left-to-right diagonal (3) 0.98 T right-to-left diagonal magnetic field. The resulted pattern from each set of parameters is shown in blue color with the unit cell displaying in a darker yellow or blue color in the figure.
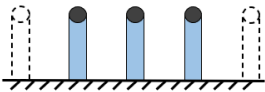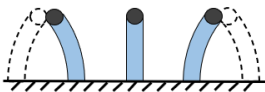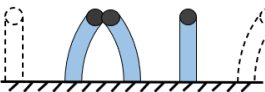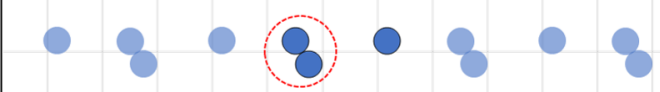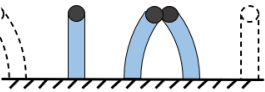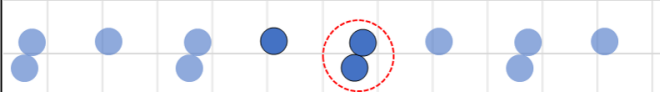
Stage	Desired mechanism	Magnetic field B	Pillar positional arrangement
0		$B = 0$ T	
1		→	
2		↑	
3		↑	

Fig. 7. Results of the parameter search for three-stage pairing problem.

The results showed that multistage contact is possible with the combination of designed initial arrangement of the pillar arrays and specific magnetic field conditions. This preliminary system required only a simple magnetic field that is directed to only one direction at a time to generate three-stage paring behavior. In this case, the control of magnetic field is expected to be rather simple. However, more advanced development in the control of magnetic field is certainly necessary to create a practical device in the future.

V. CONCLUSION

This study developed methods for the simulation and parameter optimization of a system of pillar arrays with magnetic tips. The simulation is based on the minimum total potential energy principle where the positions of the magnetic pillar tips are found at the minimum total sum of the potential energies due to the magnetic dipole moment, the elastic deformation, and the contact stress. The C++ simulation program with the steepest descent method as the computational method could successfully find the final tip position of pillar arrays. The results showed pair and line patterns correlating with the results from the actual experiments.

Machine learning process is implemented through CMA-ES as an alternative for the simulation of pillar behavior and in the parameter optimization process to optimize the pillar pitch and search for the parameters that allow multi-stage paring. The method could successfully obtain the preliminary results: (1) the maximum size of pillar pitch where two pillars contact at a given magnetic field strength and (2) the combinations of initial pillar positional arrangement and magnetic field conditions that allow simple three-stage paring of pillar arrays.

Even though the investigation of pillar behaviors through simulations and machine learning process is indeed more efficient than that of the practical experiments, the amount of time consumed (the computational cost) is still a main limitation for this method. As large number of generations are necessary to obtain accurate results in addition to the fact that the execution time increases significantly when more pillar elements are added into the array, solving problems with more complex pillar patterns that require a large unit cell could take tremendous amount of time.

Future development in the algorithm is essential to lessen the effects of these limitations so that we can utilize the machine learning to its full potential to realize our final goal of designing and controlling the behavior of a large mechanical system of pillar arrays as well as other magnetically controllable 3D or 4D printed structures [17]–[20].

REFERENCES

[1] G. Raemdonck, et al. "Routine Proteome Analysis Using 50-cm Micropillar Array Columns," Eng. Biotechnol. News, vol. 39, no. 8, pp. 54–56, 2019.

[2] L. Trichet, et all. "Evidence of a large-scale mechanosensing mechanism for cellular adaptation to substrate stiffness," Proc. Natl. Acad. Sci. U.S.A., vol. 109, no. 18, pp. 6933–6938, 2012.

[3] H. Izadi, N. Dogra, F. Perreault, C. Schwarz, S. Simon, and T. K. Vanderlick, "Removal of Particulate Contamination from Solid Surfaces Using Polymeric Micropillars," ACS Appl. Mater. Interfaces, vol. 8, no. 26, pp. 16967–16978, 2016.

[4] S. Hanasoge, P.J. Hesketh, and A. Alexeev, "Microfluidic pumping using artificial magnetic cilia," Microsyst. Nanoeng., vol. 4, no.1, pp. 1–9, 2018.

[5] H. Gu, et al. "Magnetic cilia carpets with programmable metachronal waves," Nat. Commun., vol. 11, no.1, pp. 1–10, 2020.

[6] K. Morton, O. K. Tsui, C.-K. Tung, J. C. Sturm, S. Y. Chou, and R. Austin, "The anti-lotus leaf effect in nanohydrodynamic bump arrays," New J. Phys., vol. 12, 085008, 2010.

[7] X. Wu, et al. "Hierarchical biointerfaces with lotus leaf-like topography for high efficient capture of circulating tumor cells," Mater. Res. Express, vol. 6, 085404, 2019.

[8] A. Geim, et al. "Microfabricated adhesive mimicking gecko foot-hair," Nature Mater., vol. 2, pp. 461–463, 2003.

[9] A.Y. Stark, I. Badge, N.A. Wucinich, T.W. Sullivan, P.H. Niewiarowski, and A. Dhinojwala, "Surface wettability plays a significant role in gecko adhesion underwater," P. Natl Acad. Sci. USA, vol. 110, no. 16, pp.6340–6345, 2013.

[10] F. Tsumori, A. Saijou, T. Osada, and H. Miura, "Development of actuation system for artificial cilia with magnetic elastomer," Jpn. J. Appl. Phys., vol. 54, 06FP12, 2015.

[11] F. Tsumori, R. Marume, A. Saijou, K. Kudo, T. Osada, and H. Miura, "Metachronal wave of artificial cilia array actuated by applied magnetic field," Jpn. J. Appl. Phys., vol. 55, 06GP19, 2016.

[12] R. Marume, F. Tsumori, K. Kudo, T. Osada, and K. Shinagawa, "Development of magnetic-field-driven artificial cilium array with magnetic orientation in each cilium," Jpn. J. Appl. Phys., vol. 56, 06GN15, 2017.

[13] H. Shinoda and F. Tsumori, "Development of Micro Pump Using Magnetic Artificial Cilia with Metachronal Wave," 2020 IEEE 33rd International Conference on Micro Electro Mechanical Systems (MEMS), Vancouver, BC, Canada, pp. 497–500, 2020.

[14] K. Maeda, H. Shinoda, and F. Tsumori, "Miniaturization of worm-type soft robot actuated by magnetic field," Jpn. J. Appl. Phys., vol. 59, no. SI, 2020.

[15] S. Gaysornkaew and F. Tsumori, "Active control of surface profile by magnetic micropillar arrays," Jpn. J. Appl. Phys., vol. 60, SCCL02, 2021.

[16] N. Hansen, "The CMA evolution strategy: A tutorial," arXiv preprint arXiv:1604.00772, 2016.

[17] F. Tsumori, H. Kawanishi, K. Kudo, T. Osada, and H. Miura, "Development of three-dimensional printing system for magnetic elastomer with control of magnetic anisotropy in the structure," Jpn. J. Appl. Phys., vol. 55, no. 6S1, 2016.

[18] S. Azukizawa, H. Shinoda, K. Tokumaru, and F. Tsumori, "3D Printing System of Magnetic Anisotropy for Artificial Cilia," J. Photopolym. Sci. Technol., vol. 31, no. 1, pp. 139–144, 2018.

[19] H. Shinoda, S. Azukizawa, K. Maeda, and F. Tsumori, "Bio-Mimic Motion of 3D-Printed Gel Structures Dispersed with Magnetic Particles," , Electrochem. Soc., vol. 166, no. 9, 2019.

[20] S. Azukizawa, H. Shinoda, and F. Tsumori, "4D-Printing System for Elastic Magnetic Actuators," 2019 IEEE 32nd International Conference on Micro Electro Mechanical Systems (MEMS), 2019.

[21] F. Tsumori, N. Miyano, and H. Kotera, "Development of Micro Actuator using Magnetic Powder and Elastic Material (First Report) -Theoretical Formulation of Magnetic Force Applied to Micro Particle-," J. Jpn. Soc. Powder Powder Metallurgy, vol. 56, no.3, pp. 127–132, 2009. [in Japanese].

[22] F. Tsumori, N. Miyano, and H. Kotera, "Development of Micro Actuator using Magnetic Powder and Elastic Material (Second Report) -Development of Simulation and Design System-," J. Jpn. Soc. Powder Powder Metallurgy, vol. 56, no. 3, pp. 133–136, 2009. [in Japanese].

[23] R.S. Paranjpe and H.G. Elrod, "Stability of chains of permeable spherical beads in an applied magnetic field," Journal of applied physics, vol. 60, no. 1 , pp.418–422, 1986.

[24] H. Hertz, "On the contact of rigid elastic solids and on hardness," In: Miscellaneous Papers, Chapter VI, 1896, pp.163–183.

[25] H.B. Curry, "The method of steepest descent for non-linear minimization problems," Quarterly of Applied Mathematics, vol. 2, no. 3, pp.258–261, 1944.

[26] M. Shibata, "cmaes", PyPI, 2021. [Online]. Available: https://pypi.org/project/cmaes/. [Accessed: 10- Mar- 2021].

[27] T. Akiba, S. Sano, T. Yanase, T. Ohta, and M. Koyama, "Optuna: A Next-generation Hyperparameter Optimization Framework," Proceedings of the 25th ACM SIGKDD International Conference on Knowledge Discovery & Data Mining, pp. 2623–2631, 2019.